Received: 30 July 2021 Revised: 8 November 2021 Accepted article published: 18 November 2021 Published online in Wiley Online Library:

(wileyonlinelibrary.com) DOI 10.1002/pi.6326

A systematic study of temperature-dependent cationic photopolymerization of cyclic esters

Yazgan Mete, Patrick Knaack and Robert Liska*

Abstract

The polymerization of cyclic esters to form polyesters is a thoroughly investigated topic and can be performed via anionic, cationic or metal-mediated techniques. While there have been attempts to apply light-induced on-demand initiation techniques, in most investigations photobase generators are used. In this work the focus lies on photoacid generators, which – contrary to many photobase generators – are easily stored, thermally stable, reactive, less sensitive towards water and oxygen inhibition and commercially available in various forms. However, in most cases the low reactivity of the monomers requires long polymerization times. Therefore, this study provides a basic study of the temperature-dependent cationic photopolymerization of cyclic esters and shows that polyesters can be formed in less than 5 min of irradiation at elevated temperatures and without solvents, leading to highly crystalline products. In addition, the temperature-dependent crystallinity, molecular weights and dispersities of the polymers are investigated and presented.

Keywords: biodegradable polymers; cyclic esters; photo-DSC; cationic photopolymerization; STA

INTRODUCTION

Cyclic esters are a class of monomers that have been thoroughly investigated and deployed in polymerization reactions. The main reason for this interest is the biocompatible and biodegradable character of the formed polyesters, which fulfill many criteria for biomedical and clinical applications. In particular, polycaprolactone and polylactide have been intensively studied and, among other cyclic esters, can be obtained via anionic,[1–8] cationic[7,8] or metal-mediated[9–11] polymerization. These techniques also allow the preparation of polymers with distinct and controlled molecular weights and very low dispersities. While the four-, six- and seven-membered cyclic esters are known to readily undergo ring-opening polymerization, the five-membered rings have long been considered to be challenging for thermodynamic reasons and low ring-strain energy.[12] However, since then successful polymerizations have been performed with different initiating systems.[1,13] Hong and Chen even took a step further and showed that the polymer can be fully recycled back to the starting material.[1] The cationic polymerization of cyclic esters has been reported using a variety of acids, including trifluoromethanesulfonic acid,[14] phosphoric acid,[15] methane/benzene sulfonic acid[16] or HCl·Et_2O.[17] Smaller cycles such as propiolactone are polymerized with enzymes,[18] Lewis acids[19] or perchloric acid[20] in literature. In particular, in the case of β-butyrolactone (βBL), the tacticity of the polymer is crucial, since isotactic compounds appear highly crystalline and atactic ones do not. Efforts to introduce more control over tacticity led to the development of yttrium,[21] zinc,[22] tin[23] or chromium based[24] compounds. Perfectly isotactic polymers are mainly produced by biotechnological routes, which are costlier.[24]

The formation of polyesters using cationic photopolymerization is rarely found. One example is shown by Sangermano *et al.*, who integrate degradable ester groups into epoxy networks by adding ε-caprolactone (εCL).[25] Barker and Dove also photopolymerize εCL as well as δ-valerolactone (δVL) using triarylsulfonium salts as photoinitiator.[26] A visible-light regulated photoacid generator (PAG) is deployed by Fu *et al.*,[27] while Li *et al.* present the use of a Zn(II) complex which exhibits different initiation kinetics depending on the selected wavelength.[28] The polymerization of εCL as well as δVL using not only UV light but also extending the range to visible light was recently performed by Yağci and coworkers. In their work diphenyliodonium salts combined with benzylic alcohol and various electron-transfer sensitizers were deployed.[29] The good compatibility of onium salts with a variety of sensitizers[30–33] creates the possibility to work with higher wavelengths and hence more environmentally friendly light sources.

In general, two different mechanisms are observed when the polymerization is performed via acid catalysis – either the conventional active-chain-end (ACE) mechanism or the activated monomer (AM) mechanism with an alcohol as initiator (Fig. 1). In the ACE mechanism the oxonium ion is attacked by a monomer. The AM mechanism occurs in the presence of an alcohol, which intercepts the growing polymer chain.[17,34,35]

---

* Correspondence to: R Liska, Institute of Applied Synthetic Chemistry, TU Wien, Getreidemarkt 9/163 MC, 1060 Vienna, Austria. E-mail: robert.liska@tuwien.ac.at

Institute of Applied Synthetic Chemistry, TU Wien, Vienna, Austria

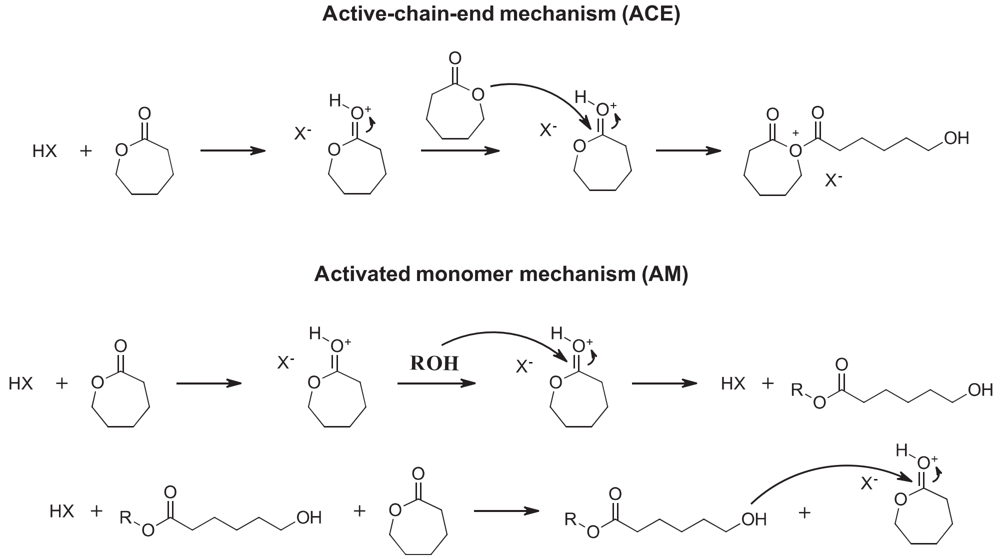

Figure 1. ACE and AM mechanisms of the acid catalyzed polymerization of ε-caprolactone.

The ACE mechanism often leads to a significant quantity of cyclic products, since backbiting and cyclization can occur. This decreases the control over the reaction and the polymer end-groups. Adding alcohols as initiator and shifting the polymerization towards an AM mechanism removes the active center from the growing chain and linear products are obtained.[34] Reports also confirm an acceleration of the reaction upon addition of alcohols to onium salt initiated systems.[35]

Increasing the polymerization rate is an important aspect, since with most initiating systems the polymerization of cyclic esters is performed over several hours. A very straightforward and convenient approach to increase the reaction speed is to perform the polymerization at high temperatures. The accelerated reaction not only leads to high yields of polyester in a very short time, but also opens up new possibilities to use cyclic esters in advanced applications. One of them is 3D printing, where complex, precise and individual polymer structures can be formed via photopolymerization. However, in order to enable the deployment of less reactive or highly viscous monomers the use of a technology called hot lithography is necessary. In this specific technique, monomers can be heated to 120 °C and their low reactivity can be overcome. Various publications have already shown the benefits of the increased printing temperature.[36–39] The 3D printing of polyesters is usually performed by preparing a polyester and modifying it with appropriate end-groups for radical polymerization. Another possibility is to deploy the polymer as a filament in the fused-deposition modeling process. In order to directly deploy the cyclic esters and synthesize the polyester during the printing, a high reactivity of the monomers and an appropriate initiating system is needed. Therefore, the temperature-dependent photopolymerization of different cyclic esters (Fig. 2) was analyzed in this study to determine an optimal temperature range for the hot lithography process. Also, since the reactivity is highly dependent on the size of the cycle, different compounds were tested, compared and it was determined whether the reactivity could be increased by high temperatures.

EXPERIMENTAL

Materials and general methods

Tert-butyldiphenyliodonium tetrakis(perfluoro-*t*-butyloxy)aluminate (I-AL) (Synthon; Bitterfeld-Wolfen; Germany), *γ*-valerolactone (*γ*VL) (TCI; Eschborn; Germany), cyclooctanone (TCI) and propiolactone (PL) (Abcr; Karlsruhe; Germany) were purchased from

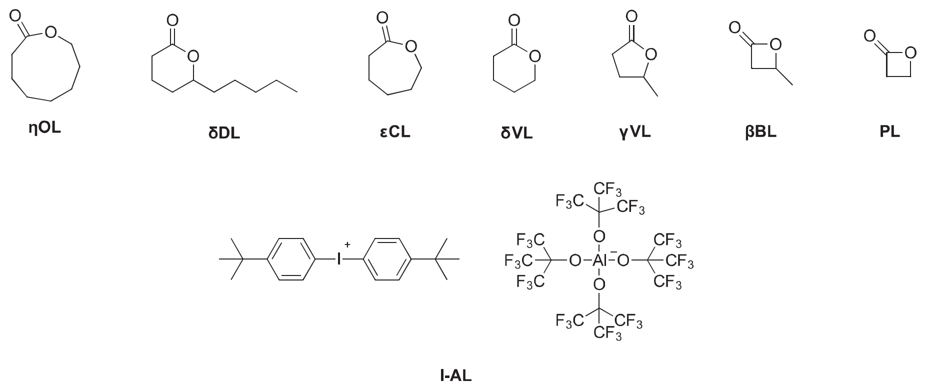

Figure 2. The tested cyclic esters *η*-octalactone (*η*OL), *δ*-decalactone (*δ*DL), ε-caprolactone (εCL), *δ*-valerolactone (*δ*VL), *γ*-valerolactone (*γ*VL), *β*-butyrolactone (*β*BL) and propiolactone (PL) and the deployed PAG *tert*-butyldiphenyliodonium tetrakis(perfluoro-*t*-butyloxy)aluminate (I-AL).

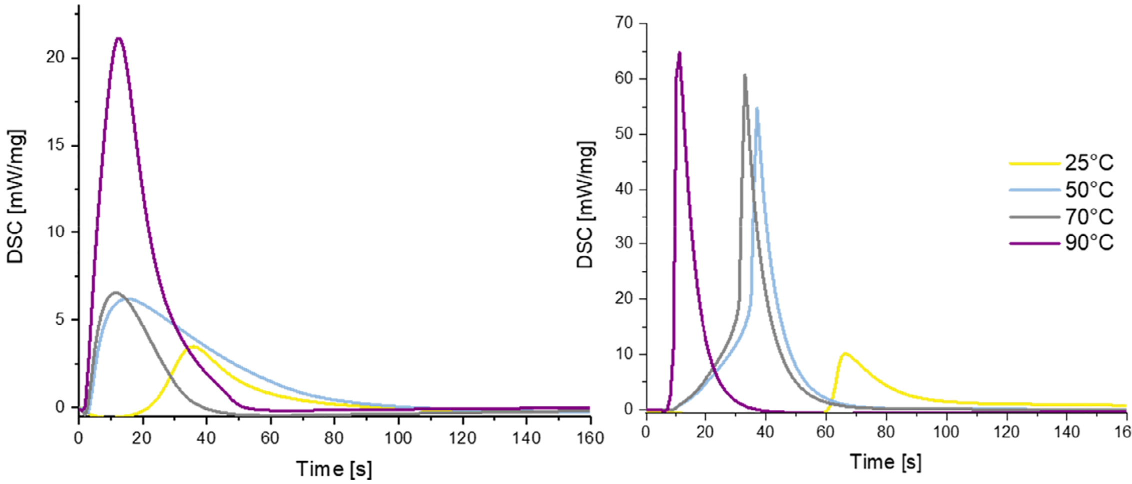

Figure 3. Photo-DSC measurements of PL (left graph) and *β*BL (right graph) cured with 0.5 mol% I-AL at different temperatures.

the respective companies and used as received. The cyclic esters *δ*VL and *β*BL were distilled prior to use and stored over molecular sieves. εCL (TCI) was dried over molecular sieves.

NMR analysis was performed with a Bruker Avance at 200 MHz for ^{1}H NMR and at 50 MHz for ^{13}C NMR. Chemical shifts were referenced to the solvent peak ($CDCl_3$) in parts per million. The peak multiplicities are described as s (singlet), d (doublet), t (triplet) or m (multiplet).

Synthesis of *η*-octalactone

The synthesis was performed based on literature reports.[40] Cyclooctanone (6.5 g, 51 mmol) was dissolved in dichloromethane (100 mL) at room temperature and 3-chloroperoxybenzoic acid (70%, 21.7 g, 88 mmol) was added in several portions while stirring. After stirring for 5 days, the white precipitate was filtered off and water was added to quench the reaction. The organic phase was extracted with $Na_2S_2O_3$, $NaHCO_3$ and H_2O and then dried with Na_2SO_4. The solvent was removed *in vacuo* and the crude product was purified via column chromatography (petroleum ether:ethyl acetate, 95:5) yielding a clear liquid (25% of theory).

^{1}H NMR (400.1 MHz, $CDCl_3$, *δ*): 4.28 (t, 2H, $–CH_2–O–$), 2.28 (t, 2H, $–CH_2–C{=}O$), 1.76–1.67 (m, 4H, $–CH_2–$), 1.67–1.59 (m, 2H, $–CH_2–$), 1.5–1.38 (m, 4H, $–CH_2–$). ^{13}C NMR (100.6 MHz, $CDCl_3$, *δ*): 175.7 (C4), 64.4 (C2), 42 (C2), 35.5 (C2), 29.4 (C2), 27.7 (C2), 27.2 (C2), 25.7 (C2), 25.0 (C2).

Photo-DSC

The photo-DSC analysis was performed on a Netzsch DSC 204 F1 device, coupled with an OmniCureTM series 2000 broadband Hg lamp as light source. The analyzed formulations contained the respective monofunctional cyclic ester and 0.5 mol% of I-AL as photoinitiator. From each formulation three identical samples were irradiated for 5 min with filtered UV light (320–500 nm). The light intensity was set to 67 mW cm^{-2} on the sample surface and the temperature during irradiation was kept at 25, 50, 70, 90 or 120 °C. The calorimetric data was only analyzed for the polymerization of PL and *β*BL, since larger rings only showed very low exothermic behavior. For each condition and formulation, the first two samples were dissolved and analyzed immediately after irradiation via NMR and gel permeation chromatography (GPC), to prevent any interference of the dark reaction. One sample was stored for at least 24 h before simultaneous thermal analysis (STA) was performed to determine melting point and crystallinity of the polyesters.

Gel permeation chromatography (GPC)

For GPC analysis the cured samples in photo-DSC crucibles were dissolved in tetrahydrofuran (THF) (about 5 mg mL^{-1}) containing 0.5 mg mL^{-1} butylated hydroxytoluene as flow marker and stabilizer and transferred into GPC vials via syringe filters. The measurements were conducted with a Malvern Viscotek TDA device equipped with three columns, which are connected in series, a

Table 1. Photo-DSC and STA of PL and *β*BL cured with 0.5 mol% I-AL

	t_{max} (s)		t_{95} (s)		Area (J g^{-1})	
T (°C)	*β*BL	PL	*β*BL	PL	*β*BL	PL
25	57 ± 5	35.7	195 ± 6	90	223 ± 24	105.6
50	31 ± 3	15.5 ± 0.24	50 ± 2	73 ± 11	621 ± 19	240 ± 66
70	11 ± 0.3	16.5 ± 3.8	30 ± 2	54.3 ± 15	548 ± 45	260 ± 95
90	6 ± 0.1	12.4 ± 0.41	21 ± 0.5	32.7 ± 1.89	486 ± 11	374 ± 25

The values for t_{max} (time to the maximum of heat development), t_{95} (time to 95% of heat development) and the area of the peaks (total polymerization heat) with the respective standard deviations were determined by measuring three samples at each temperature.

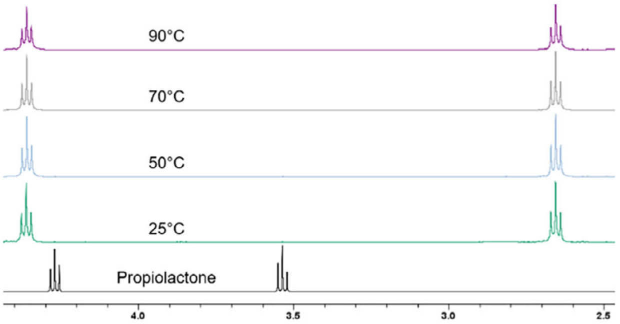

Figure 4. NMR comparison of PL and the polymers thereof analyzed immediately after 5 min of irradiation at different temperatures.

UV Detector Module 2550 for TDA 305 and a Viscotek SEC-MALS 9 light scattering detector. The molecular weight was evaluated using conventional calibration with polystyrene standards (375–177 000 Da).

Simultaneous thermal analysis (STA)

The analysis was performed with an STA 449 F1 Jupiter device from Netzsch. With this method, a temperature ramping DSC is measured simultaneously with a thermogravimetric analysis. Samples which have been previously polymerized via photo-DSC, according to the description in the section Photo-DSC, were used for the experiments. To ensure full conversion and crystallization, the samples were stored for at least 24 h at room temperature after polymerization. After replacing the glass lids of the crucibles with pierced aluminium lids, the polymer samples were heated at a rate of 10 K min^{-1} from 25 to 200 °C under N_2 atmosphere (flow rate 40 mL min^{-1}). During the heating, the calorimetric information as well as gravimetric changes were recorded and subsequently analyzed with the Netzsch Proteus thermal analysis software. To calculate the crystallinity the melting enthalpy was compared to literature values for 100% crystalline polymers.[24]

RESULTS AND DISCUSSION

Synthesis of η-octalactone

The nine-membered cyclic ester η-octalactone/8-octanolide (ηOL) was prepared starting from cyclooctanone by performing a Baeyer–Villiger oxidation reaction. The procedure was based on the description by van der Mee *et al.*[40] Cyclooctanone was dissolved in dichloromethane and an excess of *m*-chloroperoxobenzoic acid was added in portions while stirring. The reaction mixture was stirred for 5 days, since the oxidation proceeds very slowly with larger cycles compared to smaller cycles such as cyclohexanone. The literature report even suggests stirring the mixture for 13 days to increase conversion. After synthesis and work-up, the crude product was purified via column chromatography and obtained in a yield of 25%.

Reactivity analysis of cyclic esters via photo-DSC

The investigation of the cationic photopolymerization of cyclic esters was first performed via photo-DSC analysis. For this purpose, different cyclic esters were selected and polymerized using I-AL as the PAG (Fig. 2), without the addition of a co-initiator. All polymerizations were conducted with a Netzsch photo-DSC device coupled to an OmniCure Hg lamp with a spectral range of 320–500 nm as the light source. The light intensity was set to 67 mW cm^{-2} on the sample surface. For analysis the samples were weighed in a crucible, placed in the designated position and irradiated at the selected temperature. An empty crucible was used as a reference. Using the recorded heat of polymerization as a function of time, t_{max} (time until the maximum heat development is reached), t_{95} (time to 95% of heat development*)* and the area of the peaks (total polymerization heat) were determined.

The most important focus of the study was the temperature dependence of conversion and molecular weight. Therefore, all samples were irradiated for 5 min at the respective temperature and then immediately quenched. A fast quenching of the polymerization was necessary since a dark reaction was observed which proceeded after the irradiation source was turned off. All polymerizations were conducted in bulk and no solvent was needed, since the initiator (0.5 mol% I-AL) showed excellent solubility in all monomers.

The study revealed very different results for the tested compounds. The six- and seven-membered cycles did not show any significant exothermic behavior during polymerization and therefore the calorimetric data is not presented. While the six-membered compound γVL did not show any polymerization at all with the given conditions and initiator, the nine-membered ηOL as well as the six-membered δ-decalactone (δDL) only partly oligomerized at very high temperatures. The irradiation of ηOL delivered a conversion of 24% at 120 °C with a molecular weight of 2.2 kDa after 5 min. Also, the heat of polymerization decreased – as expected – with increasing ring size. Since the polymerization of the four-membered rings PL and βBL was highly exothermic, the recorded heat of polymerization is depicted in Fig. 3. The irradiation starts at $t = 0$ s and proceeds until 300 s. However, all reactions were already finished after approximately 100 s, even at room temperature.

Table 2. GPC and NMR analysis of βBL and PL polymerized via photo-DSC with 0.5 mol% I-AL at different temperatures; conversion via NMR was calculated using the end-groups of the polymer; GPC results were obtained using a polystyrene standard

	Conversion/NMR (%)		M_n/NMR (kDa)		M_n/GPC (kDa)		$Đ$/GPC (–)	
T (°C)	βBL	PL	βBL	PL	βBL	PL[a]	βBL	PL[a]
25	>99%		1.2	15.2	0.93	—	1.5	—
50			1.4	21.3	1.09	—	1.7	—
70			1.3	20.8	1.01	—	1.6	—
90			1.5	17.2	1.05	—	1.6	—

[a] Due to the insolubility of the poly-PL samples in THF, no GPC analysis was performed.

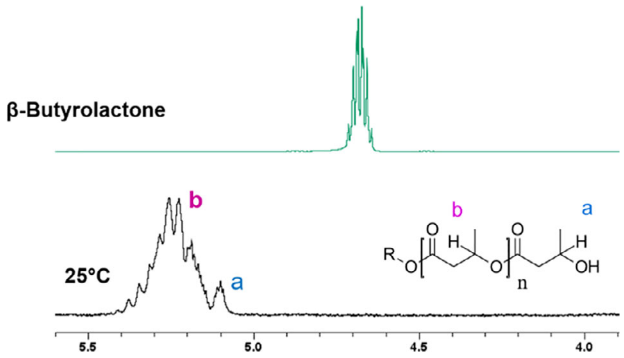

Figure 5. Example of the terminal group analysis of poly-*β*BL samples for the molecular weight determination.

While the polymerization of *β*BL (graph on the left) is slower at 25 and 50 °C and exhibits lower t_{max} values than PL (Table 1), the trend is reversed at higher temperatures. The t_{95} values, on the other hand, which show the point of time where 95% of the heat is recorded, are significantly higher for PL, since the peaks appear broader. Also, there is a retardation in the beginning at 50 and 70 °C for *β*BL, which is visible from the peak shape. A direct extraction of conversion data is not recommended, since evaporation and melting/crystallization processes are overlapping the polymerization signals.

For the photo-DSC analysis of the *β*BL and PL samples, the irradiation was conducted twice and the second irradiation phase was subtracted from the first in order to remove background signals. However, for the purpose of molecular weight and conversion determination via GPC and NMR, the same setup was repeated but the samples were removed after the first irradiation phase of 5 min and immediately dissolved in $CDCl_3$ or THF for further analysis. The NMR solvent was spiked with a small amount of pyridine to quench the reaction. NMR analysis confirms what was already expected from the DSC results. Figure 4 shows that the monomer peaks disappear at all temperatures and instead polymer peaks appear at 2.6 and 4.3 ppm.[41] However, the rather distinct shape of the peaks also indicate a small molecular weight.

The molecular weight and dispersion of the samples were determined via GPC using polystyrene standards. In addition, it was possible to detect end-groups in the NMR and calculate the degree of polymerization. In the case of PL, the polymers showed almost no solubility in THF or dimethyl sulfoxide and could therefore only be analyzed via NMR. Terminal methylene groups appear between 3.5 and 4 ppm and can be used to calculate the degree of polymerization. The summarized results are presented in Table 2.

The polymerization of PL leads to highly crystalline polymers with high molecular weights. In contrast, *β*BL forms atactic polymers, which in addition have very low molecular weights (Table 2), despite the promising photo-DSC results. NMR analysis for both monomers confirms full conversion and, in both cases, there is no clear trend visible when the temperature is increased. The most interesting aspect is that there is no correlation between initiator loading and the achieved molecular weight of the polymers. Usually, it would be expected that an initiator concentration of 0.5 mol% would lead to a polymerization degree of 200, which is exceeded in all cases for poly-PL and drastically lower for poly-*β*BL. One explanation can be derived from the ACE mechanism of the polymerization, where cyclic products can be formed due to backbiting. This would distort the molecular weight determination via end-group analysis by decreasing the number of terminal methylene groups and giving the impression of a higher degree of polymerization.

The viscous and sticky appearance of our poly-*β*BL already gives a clue about the low molecular weights of the samples and the isotactic structure. While the PAG gives no control over the tacticity, syndiotactic or predominantly isotactic products have been prepared using metal based catalysts in other studies.[21,23,24]

The low molecular weight is confirmed by GPC as well as NMR analysis, where the results are very similar. For NMR analysis, the polymer and terminal group peaks around 5 ppm (Fig. 5) were selected, based on the description of Chaber *et al.*[42] The degree of polymerization changes between 14 and 17, which is significantly lower than the expected 200 derived from the initiator concentration. The good match between NMR and GPC analysis also indicates that fewer cyclic compounds were formed.

Due to the gel-like state of the poly-*β*BL samples, no STA was performed to determine crystallinity and melting point.

The conversion of the six-membered *δ*VL and seven-membered εCL proceeds significantly slower than the four-membered cyclic esters. The slow propagation combined with the low polymerization enthalpies of −27.4 kJ mol^{-1} for *δ*VL and −28.8 kJ mol^{-1} for εCL[43] make the evaluation of the calorimetric data more difficult. At low temperatures, significantly higher irradiation times would be needed in order to record the full polymerization heat of the formulation. For both monomers, only the polymerizations at 120 °C delivered a broad peak which could be analyzed but it still has a very low height of 0.4 mW g^{-1} and an area of approximately 60 J g^{-1}. In order to compare the influence of the polymerization temperature, the irradiation time was not increased. The

Table 3. GPC, NMR and STA of εCL and *δ*VL polymerized via photo-DSC with 0.5 mol% I-AL at different temperatures; conversion via NMR was calculated using the end-groups of the polymer; GPC results were obtained using a polystyrene standard

	Conversion/NMR (%)		M_n/NMR (kDa)		M_n/GPC (kDa)		*Đ*/GPC (–)	
T (°C)	*δ*VL	εCL	*δ*VL	εCL[a]	*δ*VL	εCL[a]	*δ*VL	εCL[a]
25	41	2	1.2	—	2.86	—	1.16	—
50	41	40	2.4	0.92	4.46	2.35	1.11	1.25
70	32	33	2.7	1.7	8.21	5.61	1.12	1.19
90	42	48	2.5	2.3	15.33	7.12	1.32	1.87
120	94	99	8.8	34.3	25.45	16.3	1.9	1.94

[a] Due to the low conversion at 25 °C, the molecular weight of the sample was not determined.

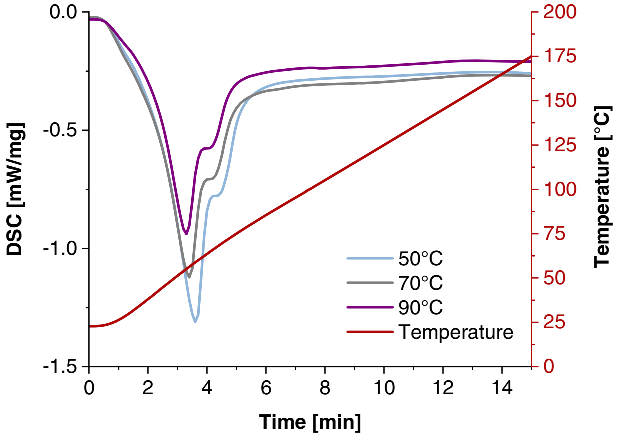

Figure 6. STA of PL for samples cured at 50, 70 and 90 °C. The temperature was increased from 25 to 200 °C at a rate of 10 K min^{-1}.

polymerization progress and molecular weights were analyzed via NMR and GPC immediately after 5 min of irradiation, analogous to all other samples.

While δVL shows first a faster polymerization than εCL, which was also observed by Yağci and co-workers,[29] the difference is reduced at higher temperatures. The crystallinity of the resulting polymers for both monomers is very high but slightly decreases with increasing temperature, which can be related to the higher molecular weights. Again, the degree of polymerization can be calculated using the terminal methylene peak of the polymer, which appears at 3.6 ppm in $CDCl_3$.[26] The M_n calculations using NMR lead to significantly higher values than the GPC analysis (Table 3). Even though the end-group analysis is usually accurate, again it can be influenced by the formation of cyclic compounds which are supposed to be formed following the ACE polymerization mechanism since no alcohol was added as initiator.[34] This means that, even though the poly-εCL appears to have a significantly higher molecular weight when analyzed via NMR, the formation of cyclic products might lead to that result, showing fewer OH groups and thus giving the impression of a higher degree of polymerization. Another crucial aspect is the occurrence of transfer reactions and transesterifications, which might be favored at higher temperature and lead to lower molecular weights for poly-δVL. In general, it was observed that δVL shows a tendency to form oligomers during storage and should be distilled prior to use. For δVL as well as εCL $Đ$ increases with increasing molecular weight. Literature suggests a reduced photoinitiator loading to decrease the dispersity.[26] A correlation between the initiator concentration and final molecular weight of the polymers could not be directly observed in any of these experiments.

Overall, all four monomers show good reactivity at elevated temperatures. While PL is also very reactive at lower temperatures, the monomer was eliminated for future 3D printing experiments because of its high price and low boiling point. The second four-membered cyclic ester βBL, on the other hand, did not form crystalline polymers like the other compounds but appeared as a highly viscous liquid, due to the low molecular weight and no control over the tacticity[44] of the methyl groups. While δVL is slightly more reactive than εCL at ambient temperatures, the difference diminishes once the polymerization is conducted at high temperatures.

Simultaneous thermal analysis (STA)

STA was performed to determine the crystallinity of the obtained polymers. For this purpose, the samples which were already cured via photo-DSC at different temperatures were directly used for STA. In order to have the same condition throughout all samples, each sample was stored for at least 24 h immediately after polymerization at room temperature. This time frame ensured full conversion due to the dark reaction for all samples and no further changes were observed after additional time. The measurements were performed with one heating cycle from 25 to 200 °C. In Fig. 6 the analysis of three poly-PL samples is shown. The melting of the samples can be clearly observed by the large peaks with two maxima. In order to calculate the crystallinity, the area of the melting enthalpy was determined and compared to the values of a 100% crystalline polymer. The values which can be found in the literature for the heat of fusion are not always consistent. Therefore, in order to compare the samples with each other, all values were taken from the same source: 151 J g^{-1} for poly-PL, 188 J g^{-1} for poly-δVL and 157 J g^{-1} for poly-εCL.[45]

As shown in Table 4, the sample cured at the highest temperature exhibits the lowest crystallinity, which can be related to the higher molecular weight of the polymer. While the correlation is clear for poly-PL, it is less obvious for the other two polymers. Even though the trend of decreasing crystallinity with increasing polymerization temperature can also be observed for poly-εCL the difference between the samples is not significant. For poly-δVL the measurement at 90 °C again disturbs the series.

All of the tested polyesters have a glass transition temperature (T_g) below 0 °C, which cannot be observed when the heating cycle is in the range 25–200 °C. The literature reports values in the range of −70 to −50 °C for poly-εCL[45–48] and poly-δVL[45,49] and −30 to −10 °C for poly-PL.[41,45]

Table 4. Melting points and calculated crystallinity values of the polymerized samples, based on the area of the melting peaks and the heat of fusion of 100% crystalline polymers

	Crystallinity (%)			Melting point (°C)		
Polymerization temperature (°C)	PL[a]	δVL	εCL	PL[a]	δVL	εCL
25	—	—	86	—	58	49.9
50	64	88	82	59/67	58	57.1
70	48	86	84	56/65	60	55.8
90	40	90	68	55/64	58	57.3
120	—	78	80	—	59	59.8

[a] PL was not polymerized at 120 °C due to its low boiling point. The samples polymerized at 25 °C could not be deployed for STA measurements.

In general, in STA measurements of crystalline materials, the transition at T_g is less prominent than the melting of the material. Also, since it was observed that crystallinity is highly dependent on the cooling process and the storage time of the material, the materials were not subjected to any further cooling or even a second heating cycle in order to determine the crystallinity.

CONCLUSION

The cationic photopolymerization of cyclic esters is less intensively investigated than polymerization using photobase generators. However, there are various PAGs which are very reactive, easy to store and commercially available, while equally convenient photobase generators are still being developed. Cyclic esters, on the other hand, are highly interesting monomers and using light-induced on-demand curing opens up new application fields. The use of PAGs leads to a successful, fast and solvent-free polymerization of various cyclic esters, where the reactivity of the monomers can be increased by applying higher temperatures. It was shown that polymerization at higher temperatures also allows the fast polymerization of monomers such as εCL or δVL, which are significantly slower than highly reactive, four-membered cycles at ambient temperatures. At the same time this study also shows the influence of the polymerization temperature on the molecular weight and crystallinity of the resulting polymers. Overall, further investigations are necessary to analyze the use of PAGs for the formation of polyesters and the use of high polymerization temperatures to accelerate the slow polymerization of abundantly used monomers such as εCL or δVL.

ACKNOWLEDGEMENTS

The authors acknowledge TU Wien Bibliothek for financial support through its Open Access Funding Programme.

CONFLICT OF INTEREST

The authors declare no financial conflict of interest.

REFERENCES

1 Hong M and Chen EY-X, *Angew Chem Int Ed* **55**:4188–4193 (2016).
2 Lohmeijer BGG, Pratt RC, Leibfarth F, Logan JW, Long DA, Dove AP *et al.*, *Macromolecules* **39**:8574–8583 (2006).
3 Brown HA, de Crisci AG, Hedrick JL and Waymouth RM, *ACS Macro Lett* **1**:1113–1115 (2012).
4 Zhang L, Nederberg F, Pratt RC, Waymouth RM, Hedrick JL and Wade CG, *Macromolecules* **40**:4154–4158 (2007).
5 Kamber NE, Jeong W, Gonzalez S, Hedrick JL and Waymouth RM, *Macromolecules* **42**:1634–1639 (2009).
6 Connor EF, Nyce GW, Myers M, Möck A and Hedrick JL, *J Am Chem Soc* **124**:914–915 (2002).
7 Penczek S, Cypryk M, Duda A, Kubisa P and Słomkowski S, *Prog Polym Sci* **32**:247–282 (2007).
8 Ottou WN, Sardon H, Mecerreyes D, Vignolle J and Taton D, *Prog Polym Sci* **56**:64–115 (2016).
9 Wu J, Yu T-L, Chen C-T and Lin C-C, *Coord Chem Rev* **250**:602–626 (2006).
10 Uhrich KE, Cannizzaro SM, Langer RS and Shakesheff KM, *Chem Rev* **99**:3181–3198 (1999).
11 Arbaoui A and Redshaw C, *Polym Chem* **1**:801–826 (2010).
12 Houk KN, Jabbari A, Hall HK and Alemán C, *J Org Chem* **73**:2674–2678 (2008).
13 Moore T, Adhikari R and Gunatillake P, *Biomaterials* **26**:3771–3782 (2005).
14 Jaipuri FA, Bower BD and Pohl NL, *Tetrahedron* **14**:3249–3252 (2003).
15 Macdonald EK and Shaver MP, *Eur Polym J* **95**:702–710 (2017).
16 Self JL, Dolinski ND, Zayas MS, Read de Alaniz J and Bates CM, *ACS Macro Lett* **7**:817–821 (2018).
17 Shibasaki Y, Sanada H, Yokoi M, Sanda F and Endo T, *Macromolecules* **33**:4316–4320 (2000).
18 Matsumura S, Beppu H, Tsukada K and Toshima K, *Biotechnol Lett* **18**:1041–1046 (1996).
19 Teranishi K, Iida M, Araki T, Yamashita S and Tani H, *Macromolecules* **7**:421–427 (1974).
20 Cerrai P, Tricoli M, Andruzzi F, Paci M and Paci M, *Polymer* **28**:831–836 (1987).
21 Amgoune A, Thomas CM, Ilinca S, Roisnel T and Carpentier J-F, *Angew Chem Int Ed* **45**:2782–2784 (2006).
22 Le Borgne A and Spassky N, *Polymer* **30**:2312–2319 (1989).
23 Kricheldorf HR and Eggerstedt S, *Macromolecules* **30**:5693–5697 (1997).
24 Zintl M, Molnar F, Urban T, Bernhart V, Preishuber-Pflügl P and Rieger B, *Angew Chem Int Ed* **47**:3458–3460 (2008).
25 Sangermano M, Tonin M and Yağci Y, *Eur Polym J* **46**:254–259 (2010).
26 Barker IA and Dove AP, *Chem Commun* **49**:1205–1207 (2013).
27 Fu C, Xu J and Boyer C, *Chem Commun* **52**:7126–7129 (2016).
28 Li M, Zhang P and Chen C, *Macromolecules* **52**:5646–5651 (2019).
29 Bener S, Yilmaz G and Yağci Y, *ChemPhotoChem* (2021). https://chemistry-europe.onlinelibrary.wiley.com/doi/pdfdirect/10.1002/cptc.202100118?download=true
30 Crivello JV and Jang M, *J Photochem Photobiol A Chem* **159**:173–188 (2003).
31 Aydogan B, Gundogan AS, Ozturk T and Yağci Y, *Macromolecules* **41**:3468–3471 (2008).
32 Bromme T, Oprych D, Horst J, Pinto PS and Strehmel B, *RSC Adv* **5**:69915–69924 (2015).
33 Crivello JV, Dietliker K and Bradley G, *Photoinitiators for Free Radical Cationic and Anionic Photopolymerisation*. Wiley, London, UK (1999).
34 Baśko M and Kubisa P, *J Polym Sci A Polym Chem* **44**:7071–7081 (2006).
35 Crivello JV and Acosta Ortiz R, *J Polym Sci A Polym Chem* **40**:2298–2309 (2002).
36 Steyrer B, Busetti B, Harakály G, Liska R and Stampfl J, *Addit Manuf* **21**:209–214 (2018).
37 Peer G, Dorfinger P, Koch T, Stampfl J, Gorsche C and Liska R, *Macromolecules* **51**:9344–9353 (2018).
38 Klikovits N, Sinawehl L, Knaack P, Koch T, Stampfl J, Gorsche C *et al.*, *ACS Macro Lett* **9**:546–551 (2020).
39 Dall'Argine C, Hochwallner A, Klikovits N, Liska R, Stampf J and Sangermano M, *Macromol Mater Eng* **218**(18):2000325 (2020).
40 van der Mee L, Helmich F, de Bruijn R, Vekemans JAJM, Palmans ARA and Meijer EW, *Macromolecules* **39**:5021–5027 (2006).
41 Cerbai B, Solaro R and Chiellini E, *J Polym Sci A Polym Chem* **46**:2459–2476 (2008).
42 Chaber P, Kwiecień M, Zięba M, Sobota M and Adamus G, *RSC Adv* **7**:35096–35104 (2017).
43 Duda A and Kowalski A, *in Handbook of Ring-Opening Polymerization*, WILEY-VCH Verlag GmbH & Co. KGaA, Weinheim, pp. 1–51 (2009).
44 Thomas CM, *Chem Soc Rev* **39**:165–173 (2010).
45 Wunderlich B, *Pure Appl Chem* **67**:1019–1026 (1995).
46 Tiptipakorn S, Keungputpong N, Phothiphiphit S and Rimdusit S, *J Appl Polym Sci* **132**:1–11 (2015).
47 Koleske JV and Lundberg RD, *J Polym Sci A* **7**:795–807 (1969).
48 Herrera D, Zamora J-C, Bello A, Grimau M, Laredo E, Müller AJ *et al.*, *Macromolecules* **38**:5109–5117 (2005).
49 Aubin M and Prud'homme RE, *Polymer* **22**:1223–1226 (1981).